Blood Supply and Vascularization of Lung Cancer, Studies by MRI and Optical Imaging

G. J. Ramniceanu[1], E. Eyal[2], I. Biton[3], N. Nevo[2], R. Margalit[4], R. Eilam-Altstadter[3], and H. Degani[1]
[1]Biological regulation, Weizmann Institute of Science, Rehovot, Israel, [2]biological regulation, Weizmann Institute of Science, Rehovot, Israel, [3]Veterinary Resources, Weizmann Institute of Science, Rehovot, Israel, [4]Immunology, Weizmann Institute of Science, Rehovot, Israel

Purpose:
Our goal is to characterize the source of blood supply and the vascular properties of human lung cancer in an orthothopic rat model using *ex vivo* optical methods and *in vivo* MRI

Introduction:
The perfusion of tumors relies upon the development of a complex and tortuous system of blood micro-vessels that provide them with both nutrients and oxygen. Frequently, however, tumor capillaries are leaky and exhibit high permeability which, in turn, leads to increased interstitial fluid pressure and decreased perfusion. Tumors in the lung, unlike tumors in other organs, can obtain their blood supply from two different systems: the pulmonary and bronchial circulations. Consequently, angiogenesis and perfusion of lung nodules may exhibit unique features. Overall, there are only few studies on lung cancer neovascularization and little knowledge is available on the involvement of the bronchial and/or pulmonary systems in lung cancer angiogenesis. The unique dual blood supply in the lung underscores the importance of utilizing orthotopic animal models in the study of lung cancer vasculature and the effects of therapy on the progression of this disease; hence, we are concentrating on establishing such rodent lung cancer models, and combining optical imaging and MRI means to monitor angiogenesis and microvascular perfusion. We have hypothesized that angiogenesis of lung cancer can rely on both systems, the bronchial and pulmonary blood vessels, either independently or through bronchio-pulmonary anastomoses. We therefore initiated investigations of the role of the two blood circulation systems in angiogenesis and function of lung cancer tumors.

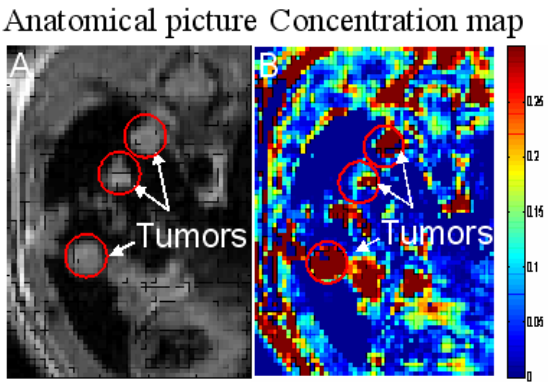

Figure 1. (A) Anatomical slice of a rat lung (T_2 weighted). Two tumor nodules are observed in the right lung (white arrows). (B) Maps of steady-state tissue GdDTPA concentration of the two nodules (white arrows).

Methods:
Animal model: Human non small lung carcinoma cells NCI-H460 were orthotopically implanted in female nude rats employing a modified procedure described by Howard *et.al.* (2).
Magnetic Resonance Imaging: Images were acquired with a 9.4 Tesla Biospec Spectrometer, equipped with a ^{1}H radiofrequency quadrature coil, 9.6 cm in diameter (Bruker, Karlsruhe Germany) employing the same pixel resolution of 0.2 X 0.2 X 1 mm^3 in all protocols. In addition we also acquired respiratory-gated RARE T_2-weighted images using the Physiograd SM 785 NMR Trigger Unit (Bruker, Karlsruhe, Germany).
We monitored contrast enhancement in the tumor nodules of rats (n=9) by continuously infusing a contrast agent at a rate of 0.525 mmol/h/kg body wt. Signal intensity in the tissues were monitored sequentially before and during infusion using 3D-GE sequence with TE/ TR/flip angle of 2.5/8/30° ms; 256x256x16 matrix; 1.28-mm slice thickness; and 5x5x2 cm^3 field of view and a temporal resolution of 3 minutes and 30 seconds.
In order to determine the tissue contrast agent concentration at steady state infusion we measured the T1 relaxation rates before and at 90 min after the start of the infusion of the contrast agent. We applied a spin echo MSME imaging sequence with a constant TE, and variable TR values.
All data analyses were performed using MATLAB programming environment (v7.0.1, MathWorks, Inc., Natick, MA). Maps of $1/T_1$ were calculated, pixel by pixel, by non linear fitting of the MR data. The steady state tissue concentration maps were determined by subtracting the pre from the steady state contrast $1/T_1$ maps taking into account GdDTPA relaxivity r_1 with the assigned value of 4.2 mM/s.
Ex vivo optical methods and histology: After anesthesia, a thoracotomy was performed to remove the thoracic cage of the rodent. In order to select perfusion through the pulmonary circulation, the heart was mobilized and the arch of the aorta was clamped to prevent blood from entering the bronchial arteries. Both superior and inferior vena cava were clamped. The left atrium was incised to prevent pressure to build up inside the vessels. A solution of 25 % diluted Indian ink in PBS was injected into the right ventricle. In order to selectively select the bronchial circulation, the heart was mobilized, the pulmonary arteries were sectioned to prevent any blood from entering the lung through the pulmonary circulation, the pulmonary veins were incised and the dye was injected into the left ventricle.
Averaged area of stained lung blood vessels were determined using Image Pro Plus software (MediaCybernetics), allowing to compare between the two lung circulation systems in both healthy lung and lung cancer tissues. In order to quantify the blood vessels' density, a user-specific sensitivity was set as the default sensitivity and was applied in all pictures. The stained area was divided by the total number of pixels contained in the picture of normal lung tissue, or by the area of the ROI in the tumor. Microscopically, hematoxylin–eosin staining of tumor sections revealed poorly differentiated cells, usually organized as a group of nodules embedded in the healthy lung parenchyma and around the bronchi, with no signs of inflammation. Most of the cells appeared viable and densely packed.

Results and Discussion:
MRI: The tumor nodules were scanned four to six weeks after implantation, when they reached a median size of 14 mm^3 (Fig 1. A) as determined from T_2 weighted images. The slowly infused contrast agent reached a steady state perfusion after approximately 30 min. Maps of T_1 relaxation times pre-contrast and at steady state infusion and of t tissue GdDTPA concentration at steady-state revealed that the contrast agent was similarly distributed within the tumor tissue (Fig 1 B). The mean concentration in the tumors was 0.3±0.3 mM in the cancerous nodules as compared to 0.08±0.02 in the muscle

	Average	±SD
Pulmonary vascular density in the periphery of tumors[#]	2.35%	1.67%
Bronchial vascular density in the periphery of tumors[#]	0.80%	0.15%
Pulmonary vascular density inside tumors	0.15%	0.38%
Bronchial vascular density inside tumors	2.72%	1.48%

Table 1. Blood vessels density of the two lung circulation systems in lung tumors of rats

Histological analysis: The density and distribution of the blood capillaries in the tumors were revealed by china ink staining of the blood capillaries throughout the whole tumor. Quantitative analysis showed significant differences between the density of capillaries in the rim and the center of the tumors stemming from the pulmonary and bronchial systems (Table 1). Overall, stained bronchial vessels were observed in the center of tumors and also in the periphery. In contrast, little or no stained pulmonary vessels were found in the center of tumors. Most of the pulmonary staining was found on the rim. Thus, both circulation systems contributed to the perfusion of peripheral regions, with the pulmonary circulation being dominant, whereas perfusion inside the tumors was dominated by the bronchial circulation.

Conclusion:
We have found that both the pulmonary and bronchial systems contribute to the vasculature and perfusion of lung cancer in the rat model system. The pulmonary derived microvessels dominate the peripheral vasculature whereas the bronchial derived microvessels dominate the vasculature inside the tumors. The total vascular density, however, was similar in both the peripheral and internal tumor regions. The MRI perfusion studies also showed similar perfusion function throughout the whole tumor, suggesting efficient and similar perfusion of microvessels derived from both systems. The perfusion appeared to be determined by concentration gradients and not by pressure gradients. This behavior is clearly different from that observed in tumors of the same cell origin implanted in the flank of nude mice (3) emphasizing the importance of orthotopic tumor models.

References: 1. Howard, R.B. *et al* Cancer Res, 51: 3274-3280, 1991. **2.** Pan, Y. *et al* Eur Surg Res, 37: 92-99, 2005. **3.** Hassid, Y. *et al*, Microvasc Res, 76: 94-103, 2008.